Development of a Retinal-Based Probe for the Profiling of Retinaldehyde Dehydrogenases in Cancer Cells

Sebastiaan T. A. Koenders,[†,#] Lukas S. Wijaya,[‡] Martje N. Erkelens,[§] Alexander T. Bakker,[†] Vera E. van der Noord,[‡] Eva J. van Rooden,[†] Lindsey Burggraaff,[∥] Pasquale C. Putter,[†] Else Botter,[†] Kim Wals,[†,#] Hans van den Elst,[⊥] Hans den Dulk,[†] Bogdan I. Florea,[⊥] Bob van de Water,[‡] Gerard J. P. van Westen,[∥] Reina E. Mebius,[§] Herman S. Overkleeft,[⊥] Sylvia E. Le Dévédec,[‡] and Mario van der Stelt*,[†,#]

[†]Department of Molecular Physiology, Leiden Institute of Chemistry, Leiden University, Leiden 2300 RA, The Netherlands

[‡]Cancer Therapeutics and Drug Safety, Division of Drug Discovery and Safety, Leiden Academic Centre for Drug Research, Leiden University, Leiden 2300 RA, The Netherlands

[§]Department of Molecular Cell Biology and Immunology, Amsterdam University Medical Centra, Amsterdam 1081 HV, The Netherlands

[∥]Computational Drug Discovery, Division of Drug Discovery and Safety, Leiden Academic Centre for Drug Research, Leiden University, Leiden 2300 RA, The Netherlands

[⊥]Department of Bio-Organic Synthesis, Leiden Institute of Chemistry, Leiden University, Leiden 2300 RA, The Netherlands

[#]Oncode Institute, Utrecht 3521 AL, The Netherlands

S *Supporting Information*

ABSTRACT: Retinaldehyde dehydrogenases belong to a superfamily of enzymes that regulate cell differentiation and are responsible for detoxification of anticancer drugs. Chemical tools and methods are of great utility to visualize and quantify aldehyde dehydrogenase (ALDH) activity in health and disease. Here, we present the discovery of a first-in-class chemical probe based on retinal, the endogenous substrate of retinal ALDHs. We unveil the utility of this probe in quantitating ALDH isozyme activity in a panel of cancer cells via both fluorescence and chemical proteomic approaches. We demonstrate that our probe is superior to the widely used ALDEFLUOR assay to explain the ability of breast cancer (stem) cells to produce *all-trans* retinoic acid. Furthermore, our probe revealed the cellular selectivity profile of an advanced ALDH1A1 inhibitor, thereby prompting us to investigate the nature of its cytotoxicity. Our results showcase the application of substrate-based probes in interrogating pathologically relevant enzyme activities. They also highlight the general power of chemical proteomics in driving the discovery of new biological insights and its utility to guide drug discovery efforts.
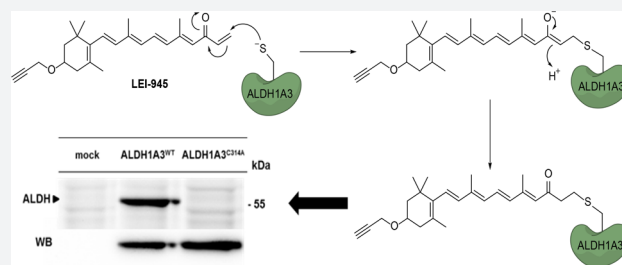
INTRODUCTION

All-trans retinoic acid (ATRA), the bioactive form of vitamin A, regulates many cellular and physiological functions, including embryonic development, immunomodulation, neuronal differentiation, and (cancer) stem cell proliferation.[1−4] Most of the cellular functions of ATRA are mediated via its binding to the retinoic acid receptor (RAR), which forms heterodimers with the retinoid X receptor (RXR). Binding of ATRA to the RAR/RXR heterodimer complex modulates gene transcription by recruiting different cofactors to the DNA-bound complex in a cell specific manner.[5,6] ATRA is essential for living organisms, and disruption of ATRA signaling leads to severe (neural) developmental defects, autoimmunity disorders, and cancer. The key function of ATRA in biological signaling implies that its cellular levels are tightly regulated.

ATRA is formed by two-step oxidation of its precursor retinol, which is taken up from the diet.[7] Retinol is converted to retinal in a reversible manner by alcohol dehydrogenases. Retinal is subsequently oxidized to ATRA by retinaldehyde dehydrogenases in an irreversible and rate limiting step. Three retinaldehyde dehydrogenases (i.e., ALDH1A1, ALDH1A2, and ALDH1A3), which belong to a superfamily of 19 aldehyde dehydrogenases (ALDHs), produce ATRA from retinal in a cell specific manner.[8,9] Noteworthy, ALDH1A1 and ALDH1A3 have also been reported as cancer stem cell biomarkers,[10] and ALDH1A1 activity may confer resistance against chemo- and radiation therapy.[11−13]
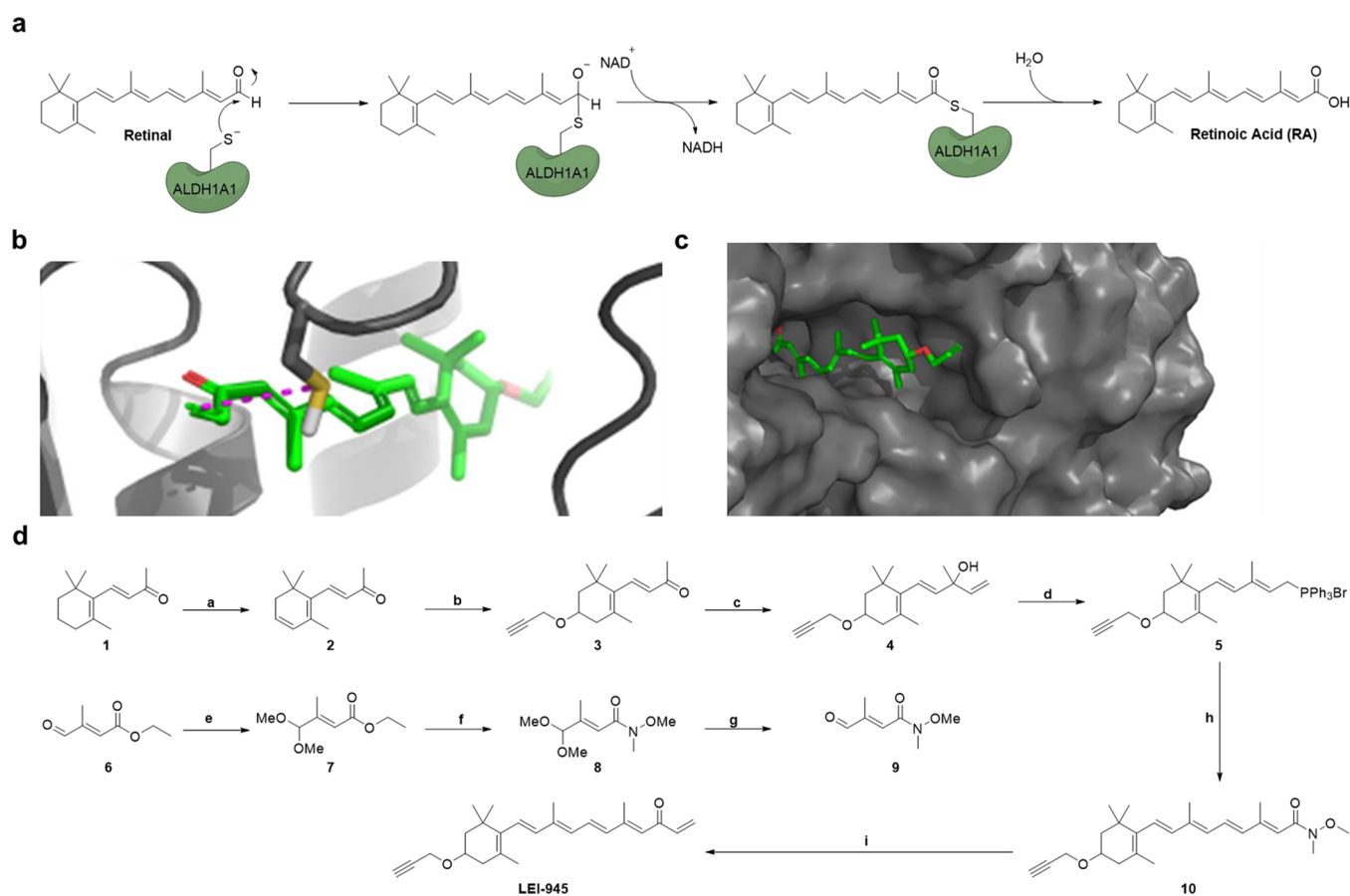
Figure 1. Design and synthesis of the retinal-based probe **LEI-945**. (a) Enzymatic conversion of retinal to retinoic acid by ALDH1A1. Nucleophilic attack of the cysteine on the aldehyde of retinal resulting in a hemithioacetal. Hydride abstraction by nicotinamide adenine dinucleotide (NAD$^+$) results in a thioester which is consequently hydrolyzed releasing the product. (b) Docking pose of retinal probe **LEI-945** in crystal structure of ALDH1A1 (PDB: 4WP7) showing the location of interaction between the vinyl ketone warhead and the catalytic cysteine (C303). (c) Docking pose of retinal probe **LEI-945** in crystal structure of ALDH1A1 (PDB: 4WP7) showing the ligation handle solvent exposed. (d) Synthesis of activity-based probe **LEI-945**. Reagents and conditions: (a) NBS, AIBN, CCl$_4$, 80 °C, 2 h, then Na$_2$CO$_3$, DMF, 81% over two steps; (b) H$_2$SO$_4$, propargyl alcohol, 4 °C, 18 h, 23%; (c) vinylmagnesium bromide, THF, 18 h, quant.; (d) PPh$_3$HBr, 18 h, 78%; (e) trimethyl orthoformate, *p*TsOH, MeOH, 2 h, quant.; (f) *N,O*-dimethylhydroxylamine hydrochloride, *i*-PrMgCl, THF, 3 h, quant.; (g) TFA, DCM/H$_2$O, 2 h, quant.; (h) 9, *n*-BuLi, THF, −78 °C to rt, 2 h, 46%; (i) vinyl magnesium bromide, THF, 2 h, 43%.

The ability to discern the contribution of specific retinaldehyde dehydrogenases to the global ALDH activity is necessary to understand the underlying biology and develop effective anticancer therapies. Retinaldehyde dehydrogenases have a variable and inducible cellular expression pattern. Their activity is regulated by protein−protein interactions and post-translational modifications.[14,15] Immunoblotting and quantitative real-time polymerase chain reaction (RT-PCR) are currently used to determine retinaldehyde dehydrogenase expression in cells, but these assays report solely on protein expression levels and not on activity.[16,17] The ALDEFLUOR assay does report on global ALDH activity levels in (cancer) stem cells. This assay uses a fluorescent aldehyde that upon oxidation to a fluorescent carboxylate remains trapped within cells. However, the ALDEFLUOR assay does not discriminate between individual ALDHs.[18] Recently developed selective fluorescent substrates report on the activity of a single enzyme but do not provide an overview of the global ALDH activity present in a biological system.[19,20] The development of chemical tools and methods to profile cellular retinaldehyde dehydrogenase activity is, therefore, important to study ATRA signaling in cancer (stem) cells and the discovery of effective molecular therapeutic strategies.

Selective ALDH inhibitors are required to study the physiological role of retinaldehyde dehydrogenases in cancer cells in an acute and dynamic matter and may serve as potential drug candidates. Most reported ALDH inhibitors, such as disulfiram, 4-diethylaminobenzaldehyde (DEAB), citral, and gossypol, however, are weakly active and/or demonstrate promiscuous behavior, which complicates the interpretation of their biological effects.[8,21] Analogues of the natural product duocarmycin have been shown to target ALDH1A1.[22] Recently, NCT-505 was developed as one of the first promising, potent ALDH1A1 inhibitors with a >1000-fold selectivity over ALDH1A3 as determined in a biochemical assay.[23] NCT-505 was cytotoxic to ovarian cancer cells and sensitized them to paclitaxel. The cellular selectivity profile and its mode-of-action have not been reported yet, which would be of importance to guide its therapeutic development.

The determination of target protein engagement and off-target activities of small molecules is an essential step in drug discovery. Activity-based protein profiling (ABPP) has become one of the key methodologies to map the interactions of inhibitors and enzymes on a global scale in living systems, such as cells and animals.[24,25] ABPP is a technology that relies on activity-based chemical probes that covalently and irreversibly
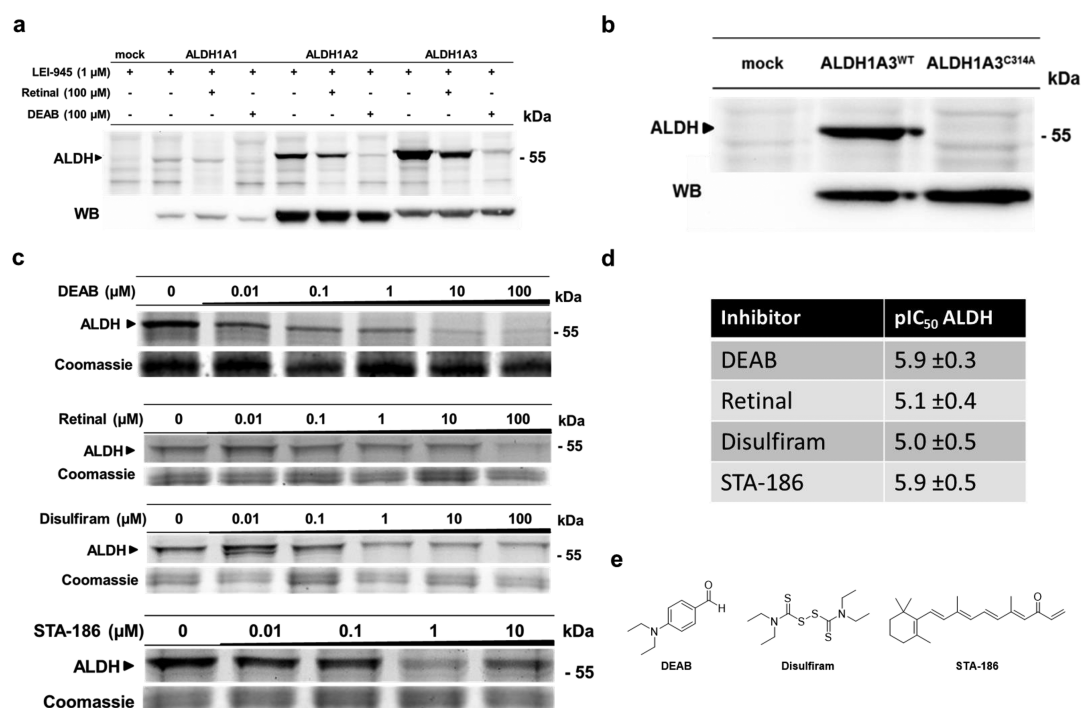
Figure 2. *In situ* labeling of ALDH by **LEI-945** and competition with inhibitors. (a) *In situ* labeling of ALDH1A1, ALDH1A2, and ALDH1A3 transiently transfected in U2OS cells using **LEI-945** (1 μM) for 1 h at 37 °C and anti-FLAG Western blot. Competition was performed with natural substrate retinal (100 μM) or general ALDH inhibitor DEAB (100 μM). (b) *In situ* labeling of ALDH1A3[WT] and mutant ALDH1A3[C314A] with **LEI-945** (1 μM) for 1 h at 37 °C and anti-FLAG Western blot. (c) *In situ* labeling of endogenous ALDH enzymes in A549 lung cancer cells with **LEI-945** (1 μM) and competition with ALDH inhibitors or natural substrate. (d) Table showing the pIC$_{50}$ values ± SD of several ALDH inhibitors as determined by competitive ABPP with probe **LEI-945** (1 μM) in three experiments. (e) Chemical structures of ALDH inhibitors used in this study.

react with the catalytic nucleophile in the active site of an enzyme in their native biological context.[26] Since this process requires a catalytically active protein, these chemical probes report on the abundance of active enzymes. ABPP enables the determination of target engagement and selectivity profiling of drug candidates in their physiological relevant environment, which enhances the therapeutic relevance of the observed interaction profile.[27−29] An activity-based probe (ABP) generally consists of an electrophilic warhead, a scaffold that recognizes the protein (family) of interest, and a fluorophore or biotin as reporter group. ABPP has found successful applications in detecting, among others serine hydrolases,[26,30] proteases,[31] kinases,[32] and glycosidases.[33] However, to date no ABP for retinaldehyde dehydrogenases has been developed, despite the fact that the catalytic mechanism employed by these enzymes during substrate processing involves a covalent intermediate.

Here, we describe the design, synthesis, biological validation, and application of the retinal-based ABP **LEI-945**, featuring a vinyl ketone warhead and an alkyne ligation handle for the introduction of reporter groups. **LEI-945** is a first-in-class probe that enables profiling retinaldehyde dehydrogenases in cancer cells. Comparative chemical proteomics with **LEI-945** explained the ability of various breast cancer cell lines to produce ATRA via specific ALDH isozymes, whereas the ALDEFLUOR assay could not. Competitive chemical proteomics using **LEI-945** was employed to determine the cellular target engagement and selectivity profile of NCT-505 in MDA-MB-468 breast cancer cells. We found that both ALDH1A1 and ALDH1A3 were inhibited by NCT-505 resulting in an overall reduced cell viability caused by a cell

cycle arrest and necrosis-induced cell death. Our results show that **LEI-945** holds promise to guide the discovery of ALDH-based therapeutics.

■ RESULTS AND DISCUSSION

Design and Synthesis of the Retinal-Based Probe LEI-945. Retinaldehyde dehydrogenases convert their substrate through nucleophilic attack of the catalytic cysteine thiol on the aldehyde yielding a hemithioacetal (Figure 1a). Hydride abstraction by nicotinamide adenine dinucleotide (NAD⁺) with concomitant deprotonation results in net dehydrogenation and formation of a thioester adduct.[8] Hydrolysis of this thioester by a water molecule leads to the formation of ATRA. We sought to take advantage of the fact that covalent enzyme–substrate intermediates emerge during catalysis by designing an ABP based on the structure of retinal. We hypothesized that the aldehyde in retinal could be exchanged with a vinyl ketone to trap the nucleophilic catalytic cysteine through conjugate addition (Figure 1b). Docking of such a retinal-derived vinyl ketone into the crystal structure of ALDH1A1 (PDB: 4WP7)[34] suggested that the nucleophile (the catalytic cysteine thiol) and the electrophile (the unsaturated ketone) would be in close proximity. It pointed as well to a suitable position, which is a solvent exposed position where probe contact with the enzyme active site is negligible, for installation of a bioorthogonal ligation handle (Figure 1c). An alkyne ligation handle was selected since it minimally affects the lipophilicity and physicochemical properties of the probe.[35,36] This led to the design of **LEI-945** as a potential two-step retinaldehyde dehydrogenase ABP (Figure 1d).
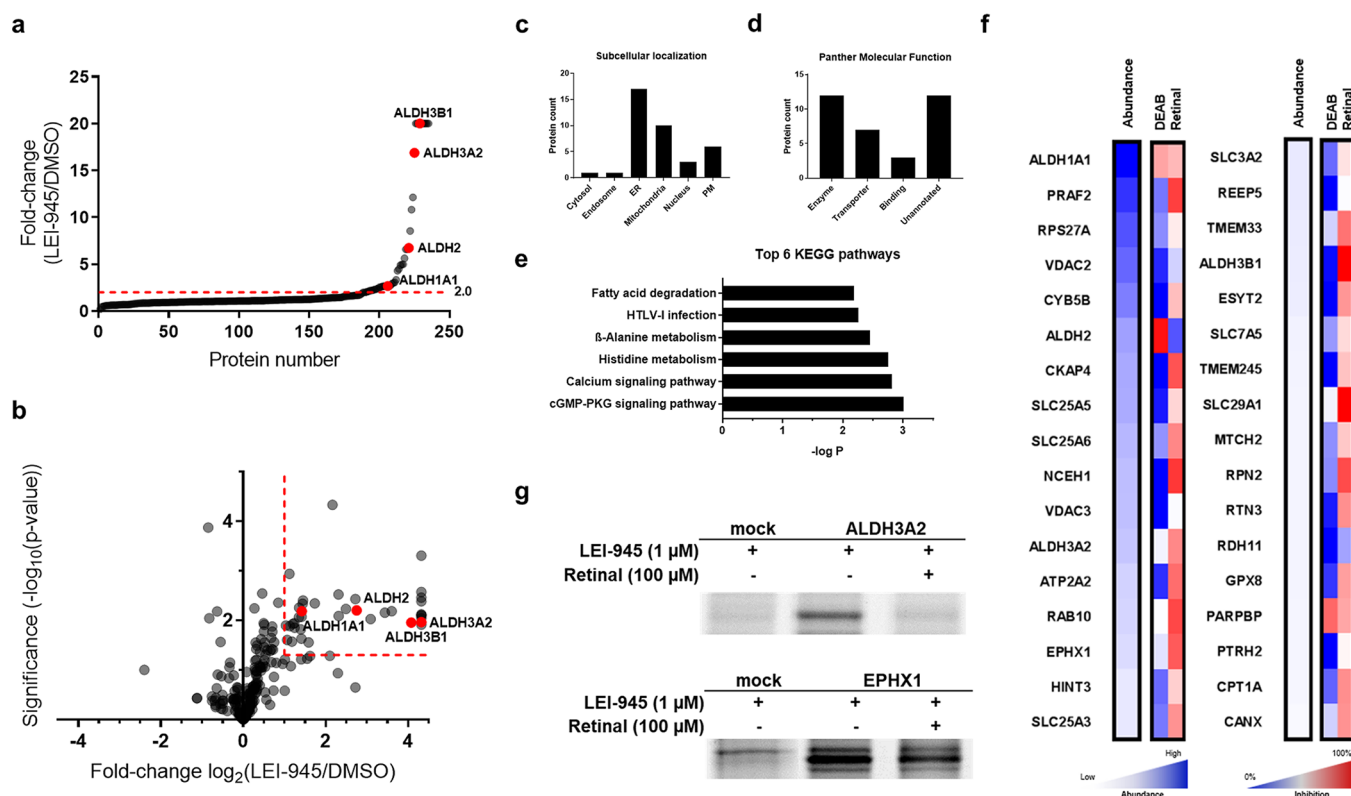
Figure 3. Proteomics data of retinaldehyde interacting proteins in A549 cells. (a) Fold-change (**LEI-945**: DMSO) plot for total proteins identified in chemical proteomics experiment with probe **LEI-945** (1 μM). Red lines indicates the threshold fold-change of 2-fold enrichment and the maximum fold-change is set at 20. Red dots represent significantly enriched ALDH enzymes. (b) Volcano plot for total proteins identified in chemical proteomics experiment with probe **LEI-945** (1 μM). Red lines indicate threshold values (fold-change >2; p-value <0.05) marking significantly enriched proteins. Red dots represent significantly enriched ALDH enzymes. (c) Subcellular localization of significantly enriched proteins as annotated by the UniProt database. (d) Molecular functions attributed to significantly enriched proteins by the Panther database. (e) Top 6 pathways enriched in the group of significantly enriched proteins as determined by screening on the KEGG database. (f) Maximum abundance (white = low; blue = high) and inhibition (blue = 0%; red = 100%) by pan-ALDH inhibitor DEAB (100 μM) and natural substrate retinal (100 μM) in competitive ABPP experiments with **LEI-945**. For parts a, b, and f, data are from $n = 4$ experiments (biological replicates). (g) *In situ* labeling of ALDH3A2 and EPHX1 transiently transfected in U2OS cells using **LEI-945** (1 μM) for 1 h at 37 °C.

LEI-945 was synthesized using a convergent synthesis scheme starting from commercially available β-ionone **1** and ethyl 3-methyl-4-oxocrotonate **6** (Figure 1d). Bromination of **1** using NBS, followed by dehydrobromination of 3-bromo-β-ionone with Na$_2$CO$_3$, afforded 3-dehydro-β-ionone **2** in 81% yield. Conjugate addition of propargyl alcohol to 3-dehydro-β-ionone **2** following a modification of the literature procedure[37] provided alkyne **3** in 23% yield. Grignard reaction of **3** and vinylmagnesium bromide quantitatively afforded tertiary alcohol **4**. Addition of triphenylphosphine hydrobromide in methanol provided phosphonium salt **5** in 78% yield.[38] Intermediate **9** required for the key Wittig reaction toward the retinal scaffold was made from commercially available ethyl 3-methyl-4-oxocrotonate **6** as follows. Treatment of **6** with trimethyl orthoformate and catalytic acid yielded acetal **7** in quantitative yield. The ester in **7** was converted into Weinreb amide **8** using *N,O*-dimethylhydroxylamine hydrochloride also in quantitative yield. The acetal in **8** was quantitatively deprotected using aqueous TFA, yielding aldehyde **9**. Phosphonium salt **5** was deprotonated at −78 °C using *n*-BuLi after which addition of aldehyde **9** and stirring at room temperature afforded compound **10**. Finally, treatment of Weinreb amide **10** with vinylmagnesium bromide furnished **LEI-945** in 20% yield over the last two steps.

Retinal-Based Probe LEI-945 Maps ALDH Activity in Living Cells. To assess whether **LEI-945** acts as a retinaldehyde dehydrogenase ABP, pcDNA3.1 plasmids containing either recombinant human ALDH1A1, ALDH1A2, or ALDH1A3 fused to a FLAG-tag were transiently transfected in human osteosarcoma U2OS cells. Living cells were treated with **LEI-945** (1 μM) in serum-free medium for 1 h, lysed, and treated with Alexa Fluor 647 dye under copper(I)-catalyzed azide−alkyne [2 + 3] cycloaddition conditions. The protein samples were resolved by sodium dodecyl sulfate polyacrylamide gel electrophoresis (SDS-PAGE) and visualized by in-gel fluorescent scanning. A fluorescent band at 55 kDa was apparent in samples harvested from three transfected cell cultures, but not in the mock-treated cells (Figure 2a). All fluorescent bands were at the same height as the signal generated by using an anti-FLAG antibody in a separate Western blotting experiment. This molecular weight matches with that of the transfected retinaldehyde dehydrogenases, suggesting that **LEI-945** indeed reacted with these in a covalent manner. Fluorescent labeling intensity was reduced by pretreatment (1 h) with retinal (100 μM) as well as with the general ALDH inhibitor, DEAB (100 μM) (Figure 2a).[39] Site-directed mutagenesis of the catalytic Cys314 into alanine in ALDH1A3, which was chosen as a representative retinaldehyde dehydrogenase, abolished labeling
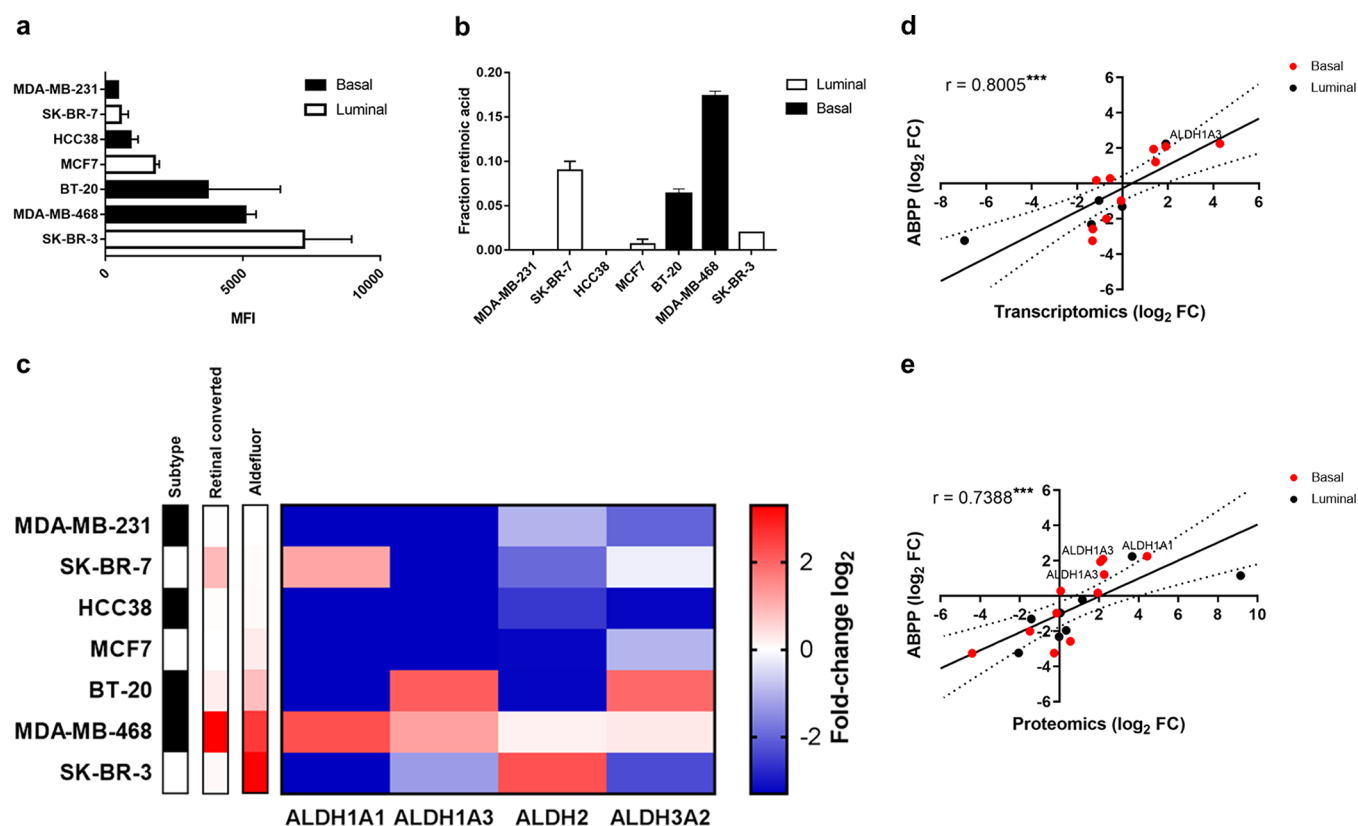
Figure 4. Profiling levels of active ALDH proteins in breast cancer cell lines. (a) Mean fluorescence intensity (MFI) of ALDH activity measured in breast cancer cell lines using the ALDEFLUOR assay. Data are represented as mean values ± SD; $N = 3$ independent experiments with each $n = 3$ experiments per group (biological replicates). (b) Retinoic acid production by breast cancer cell lines. Data represent mean values ± SD; $N = 3$ experiments (biological replicates) measured twice. (c) ALDH profiling of breast cancer cell lines using chemical proteomics. The subtype column indicates if the cell line belongs to the luminal subtype (white) or basal subtype (black). The retinal converted column shows the amount of retinal converted to retinoic acid over 4 h in a gradient from 0% (white) to 100% (red). The ALDEFLUOR column shows the ALDH activity as determined by the ALDEFLUOR assay in a gradient from low (white) to high (red). The heatmap shows the fold-change in LFQ value for each ALDH enzyme compared to the average for each ALDH enzyme. $N = 2$ independent experiments with each at least $n = 3$ experiments per group (biological replicates). (d) Correlation of transcriptomics data with ABPP data. ALDHs measured in cell lines with a basal subtype are shown as red dots, and the ones with a luminal subtype are shown as black dots and the Pearson's correlation reported for the correlation between ABPP and transcriptomics ($r = 0.8005$; $p = 0.0003$). Dotted lines represent the 95% confidence interval. (e) Correlation of proteomics data with ABPP data. ALDHs measured in cell lines with a basal subtype are shown as red dots, and the ones with a luminal subtype are shown as black dots and the Pearson's correlation reported for the correlation between ABPP and proteomics ($r = 0.7388$; $p = 0.0003$). Dotted lines represent the 95% confidence interval.

of the enzyme with **LEI-945**, whereas protein expression was not affected as determined by FLAG-tag antibody (Figure 2b). A liquid chromatography−mass spectrometry assay was developed to measure the conversion of retinal into ATRA by ALDHs. Overexpressing ALDH1A3[WT] and ALDH1A3[C314A] in U2OS in combination with this assay confirmed that Cys314 was required for the enzymatic activity of ALDH1A3 (Figure S7). Together, these data demonstrate that **LEI-945** efficiently labels ALDH1A1, ALDH1A2, and ALDH1A3 in an activity-dependent manner by forming an irreversible covalent bond with the catalytic cysteine.

To establish the potential of **LEI-945** to detect endogenous retinaldehyde dehydrogenases, we incubated the non-small-cell lung cancer cell line A549, known to express ALDH1A1,[16,40] with **LEI-945**. This yielded a fluorescent band at around 55 kDa, which could be significantly and dose-dependently reduced by preincubation with either DEAB, disulfiram,[8] STA-186, or retinal, with pIC$_{50}$ in the range 5.0−5.9 (Figure 2c,d). To find out which proteins are irreversibly and covalently labeled by **LEI-945**, a label-free chemical proteomics experiment was performed. **LEI-945** (1 μM, 1

h)-treated A549 cells were lysed and reacted with biotin-N$_3$, after which probe-labeled proteins were enriched by streptavidin bead pull-down. Subsequent trypsin digestion, protein identification, and quantification by mass spectrometry resulted in the identification of 34 significantly enriched proteins, including ALDH1A1, ALDH2, ALDH3A2, and ALDH3B1 (Figure 3a,b and Table S1). To exclude the possibility that the warhead covalently binds to reactive cysteines irrespective of recognition based on the retinal scaffold, we compared our list of 34 significantly enriched proteins with a list of the 150 most reactive cysteines. This list was compiled by Cravatt et al.[41] using ABPP with the reactive nucleophile iodoacetamide in MDA-MB-231, MCF7, and Jurkat cancer cell lines. Only two proteins (ALDH2 and RTN3) from this list were identified as interacting partners of **LEI-945**. This suggested that the scaffold of **LEI-945** confers selectivity to its binding partners and does not randomly label proteins with hyperreactive cysteines. Some of the enriched proteins have been previously reported to interact with retinoids and related lipids, such as sarcoplasmatic/endoplasmic reticulum calcium ATPase 2 (ATP2A2), ADP/ATP
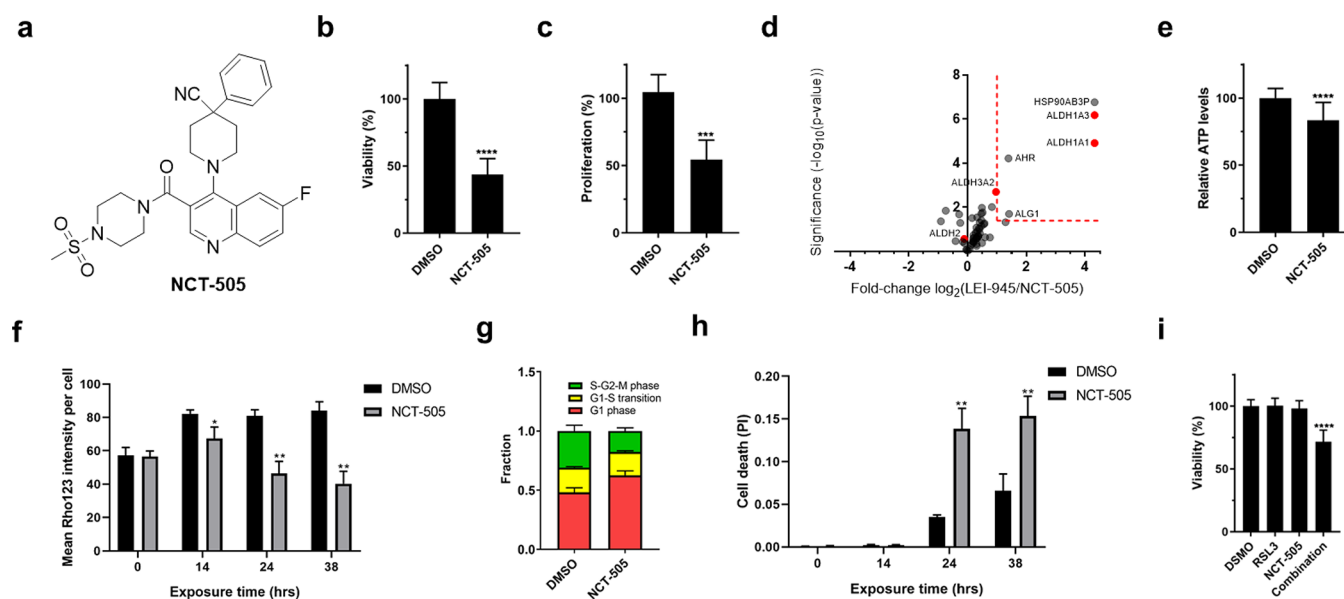
Figure 5. Physiological effects and target engagement of NCT-505 in MDA-MB-468 cells. (a) Chemical structure of ALDH1A1 inhibitor NCT-505. (b) Cell viability of MDA-MB-468 cells after treatment with NCT-505 (30 μM) for 72 h. (c) Cell proliferation of breast cancer cell lines after treatment with NCT-505 (30 μM) for 72 h. For parts b and c, data represent mean values $\pm$ SD; N = 3 biological replicates with each n = 3 experiments per group. ***P < 0.001; ****P < 0.0001; t test, two-sided. (d) Volcano plot of the *in situ* competitive ABPP experiment in MDA-MB-468 to determine off-targets of ALDH inhibitor NCT-505 (30 μM). N = 4 experiments per group (biological replicates). (e) Relative ATP levels of vehicle and NCT-505 (30 μM)-treated MDA-MB-468 cells as determined by CellTiter-Glo assay. Data represent mean values $\pm$ SD; N = 3 biological replicates with each n = 3 experiments per group. ****P < 0.0001. (f) Relative mitochondrial membrane potential ($\Delta\Psi_m$) of vehicle and NCT-505 (30 μM)-treated MDA-MB-468 cells visualized by Rhodamine 123 and measured over time. (g) Distribution over the different cell cycle phases of vehicle and NCT-505 (30 μM)-treated FUCCI-expressing cells MDA-MB-468 after 72 h. (h) Cell death profile of vehicle and NCT-505 (30 μM)-treated MDA-MB-468 cells as determined by propidium iodide (PI) staining and measured over time. For parts f−h, data represent mean values $\pm$ SD; N = 3 biological replicates with each 5 experiments per group. *P < 0.05; **P < 0.01; t test, two-sided. (i) Synergy between RSL3 (30 nM) and NCT-505 (3 μM) measured using a viability assay after 72 h of treatment. Data represent mean values $\pm$ SD; N = 3 biological replicates with each 6 experiments per group. ****P < 0.0001.

translocase 2 (SLC25A5), ADP/ATP translocase 3 (SLC25A6), voltage-dependent anion-selective channel protein 2 (VDAC2), and voltage-dependent anion-selective channel protein 3 (VDAC3).[42−45] Pathway analysis using the KEGG,[46] UniProt,[47] and Panther[48] databases and DAVID[49] analytic tools revealed that most enzymes and transporters are located in the endoplasmic reticulum and mitochondria (Figure 3c). A significant number of unannotated proteins were found, and we suggest that these proteins may be involved in retinal/retinoic acid biochemistry and biology (Figure 3d). Many proteins involved in fatty acid degradation, β-alanine, and histidine metabolism were enriched, which is in line with the proposed role of ALDH enzymes in these cellular functions (Figure 3e).[8] To investigate whether these proteins are also targeted by retinal and DEAB, we performed a competitive chemical proteomics experiment (Figure 3f). Retinal inhibited over 85% of the targets of **LEI-945**, including all identified ALDH enzymes apart from ALDH2, whereas DEAB was much more selective and reduced the labeling of only three proteins (ALDH1A1, ALDH2, and PCNA-interacting partner (PARPBP)). To validate the identified probe targets as retinoid-interacting proteins, we overexpressed recombinant ALDH3A2 and epoxide hydrolase 1 (EPHX1) as representative examples in U2OS cells and fluorescently labeled them with **LEI-945** (1 μM). Competition with retinal (100 μM) confirmed their ability to bind retinoids (Figure 3g). Taken together, these data show that **LEI-945** enables the detection of various retinaldehyde dehydrogenases and other retinoid-interacting proteins in living human cells. Having

established the efficacy and specificity of **LEI-945**, the probe was subsequently used in comparative and competitive ABPP studies as detailed in the next sections.

LEI-945 Reveals Distinct ALDH Activities in Cells of Different Breast Cancer Subtypes. ALDH activity in breast cancer cells has been linked with chemo- and radiotherapy resistance.[13] For example, the presence of ALDH1A1 has been found to correlate with resistance in cancer tissue toward cyclophosphamide, and the expression of ALDH1A3 is associated with poor clinical outcome in breast cancer.[11,12,17,50,51] To determine whether **LEI-945** can be used to profile the activities of these ALDHs in breast cancer cell lines, a panel of seven breast cancer cell lines was selected ranging from aggressive basal origin (MDA-MB-231, BT-20, MDA-MB-468, and HCC38) to less aggressive luminal origin (SK-BR-7, MCF7, and SK-BR-3).[52] Their general ALDH activity was measured using the ALDEFLUOR assay.[53] Based on this assay the breast cancer cell lines were divided into two groups: ALDH^{high} (BT-20, MDA-MB-468, and SK-BR-3) and ALDH^{low} (MDA-MB-231, SK-BR-7, HCC38, and MCF7) (Figure 4a). The two groups did not correlate with the breast cancer subtype.

Next, we determined the capability of the breast cancer cell lines to convert retinal into ATRA by liquid chromatography/mass spectrometry. Retinal (10 μM, 1 h)-treated cells were lysed and the lipids extracted after which the unique UV absorption of the retinoids relative to other metabolites was used to determine to which extent retinal was converted (Figure 4b). The results of the ALDEFLUOR assay (Figure

4a) did not correlate with the ability of cells to produce ATRA from retinal. For example, while MDA-MB-468 and SK-BR-3 were both classified as ALDH^{high}, only MDA-MB-468 cells produced significant amounts of ATRA. We hypothesized that ABPP using **LEI-945** would be able to explain these apparent contradictory results by determining the levels of active retinaldehyde dehydrogenases in each breast cancer cell line.

Chemical proteomics experiments were performed with samples from all seven breast cancer cell lines using **LEI-945** (1 μM, 1 h) (Figure 4c). ALDH1A1 was found in SK-BR-7 and MDA-MB-468. ALDH1A3 was detected in BT-20, MDA-MB-468, and SK-BR-3. ALDH2 was significantly enriched in MDA-MB-231, HCC38, MDA-MB-468, and SK-BR-3. ALDH3A2 was identified in MDA-MB-231, SK-BR-7, BT-20, MDA-MB-468, and SK-BR-3. Comparison of the chemical proteomics data with data from transcriptomics and global proteomics experiments of these breast cancer cell lines revealed in general a high correlation with r of 0.80 and 0.74 between enzyme activity and mRNA and protein levels, respectively (Figure 4d,e). Levels of active ALDH1A1 and ALDH1A3 enzymes were higher than expected on the basis of the mRNA and protein levels, indicating that the activity of these enzymes is potentially regulated post-translationally, as was previously reported.[14,15] Active ALDH1A1 was most abundant in the MDA-MB-468 cells, whereas SK-BR-3 had high levels of active ALDH2 and no discernible levels of active ALDH1A1. Since ALDH2 does not convert retinal into retinoic acid,[54] but is an efficient oxidizer of numerous aldehydes, these data may explain the discrepancy between the ALDEFLUOR assay and the retinal conversion assay. Taken together, our data show that **LEI-945** has the ability to identify individual ALDH isozyme activities in cancer cells and report on the well-known cancer biomarkers ALDH1A1 and ALDH1A3.[10]

NCT-505 Inhibits ALDH1A1 and ALDH1A3 in MDA-MB-468 Cells. For successful drug discovery it is essential to understand the molecular and cellular mode-of-action of a drug candidate. So far, studies on the physiological effects of ALDH inhibition in cancer have been mostly performed with poorly active and/or promiscuous inhibitors, which have not been properly characterized in biological systems.[13,21,40,55,56]

This complicates the interpretation of the physiological function ascribed to a specific ALDH. Here, we used **LEI-945** to study the cellular ALDH interaction profile of the ALDH1A1 inhibitor NCT-505 (Figure 5a). First, we confirmed that NCT-505 was able to significantly reduce cell viability and proliferation of MDA-MB-468 cells, which expressed the highest levels of ALDH1A1 (Figure 5b,c). To determine the cellular target engagement and off-target activities, we performed a chemical proteomics experiment with **LEI-945** using MDA-MB-468 cells *in situ* treated with NCT-505. This competitive ABPP experiment showed that both ALDH1A1 and ALDH1A3 were inhibited by NCT-505 at the concentration used in the cell viability and proliferation assay (Figure 5d). Putative heat shock protein HSP 90-beta-3 (HSP90AB3P), the aryl hydrocarbon receptor (AHR), and chitobiosyldiphosphodolichol beta-mannosyltransferase (ALG1) were also identified as off-targets of NCT-505.

Having established the cellular retinaldehyde dehydrogenase interaction profile of NCT-505 by ABPP using **LEI-945**, we further characterized the biological effects of this dual ALDH1A1/ALDH1A3 inhibitor in MDA-MB-468 cells. NCT-505 produced a limited, but significant, reduction in

ATP levels (Figure 5e). Mitochondrial membrane potential ($\Delta\Psi_m$) upon preincubation of MDA-MB-468 cells was also reduced as assessed with Rhodamine 123, a fluorescent marker for mitochondrial activity, suggesting that mitochondrial function was altered (Figure 5f and Figure S13B). In addition, exposure to NCT-505 arrested cells in the G1 cycle as determined by fluorescent ubiquitination-based cell cycle indicators (FUCCIs) (Figure 5g and Figure S14).[57] The nuclei of the NCT-505-treated cells were highly condensed compared to vehicle-treated cells indicating dying cells, which had no Rhodamine 123 signal as well (Figure S15 and arrows in Figure S13B). A significant increase in the fraction of propidium iodide positive cells was observed in NCT-505-treated cells, which suggested that the cells underwent necrosis (Figure 5h and Figure S13A). As changes in mitochondrial morphology are a distinctive feature of ferroptosis,[58] the observed nonapoptotic cell death in combination with alterations in mitochondrial function might indicate that the cells die undergoing ferroptosis. We therefore tested whether incubation with RSL3, a compound that induces ferroptosis via inhibition of GPX4,[59,60] and inhibition of ALDH1A1/ALDH1A3 could synergistically induce cell death. MDA-MB-468 cells treated separately with ineffective, low concentrations of GPX4 inhibitor RSL3 (30 nM) or NCT-505 (3 μM) did not show any reductions in cell viability, whereas the combination led to a significant decrease in cell viability (Figure 5i) with a combination index value of 0.87 indicating synergism (Figure S16).

■ CONCLUSION

In this study we present the first rationally designed, retinal-based probe **LEI-945** specifically developed for the profiling of retinaldehyde dehydrogenases. We demonstrated that **LEI-945** inhibits ALDH1A1, ALDH1A2, and ALDH1A3 in an activity-based dependent manner via irreversible covalent reaction of the catalytic cysteine and is able to detect endogenously expressed ALDH isozyme activities in various (breast) cancer cells, but also for the identification of retinoid-interacting proteins in living cells. To date only a few probes for oxidases have been reported[61−63] and only one retinoid-based probe.[64] This retinyl ester-based probe labeled two retinyl ester processing enzymes in retinal pigment epithelial membrane, but did not label ALDHs.[65] To our knowledge, **LEI-945** represents, therefore, the first-in-class probe for aldehyde dehydrogenases that enables cellular profiling of ALDH activity as cancer (stem) cell biomarkers and target engagement studies for drug discovery of this target family in drug-resistant cancer cells.

LEI-945 was able to detect and compare individual active ALDH isozymes in breast cancer cell lines. The ALDH profiles generated using **LEI-945** could be used to explain the ability of certain cell lines to produce retinoic acid, where the ALDEFLUOR assay could not. It also detected levels of active ALDH1A1 enzyme in the SK-BR-7 cell line, while the ALDEFLUOR assay reported no ALDH activity. We propose that our method can be used in combination with the ALDEFLUOR assay by sorting cells based on global ALDH activity and subsequently subjecting the sorted cell populations to comparative ABPP analysis, thus, providing both qualitative and quantitative information on the levels of active ALDH enzymes in therapy-resistant cancer (stem) cells enabling a better mechanistic understanding of the underlying biology, which is ALDH isozyme-dependent.[66]

Furthermore, we showed that **LEI-945** enabled target engagement and cellular selectivity studies of the recently reported ALDH1A1 inhibitor NCT-505. Our ABPP method revealed that NCT-505 inhibits not only ALDH1A1 but also ALDH1A3, at concentrations that significantly reduced cell viability and proliferation of MDA-MB-468 cells via inhibition of mitochondrial function, cell cycle arrest in the G1 phase, and necrosis-induced cell death. The concentration used in this study is in accordance with the reported EC_{50} value derived from OV-90 ovarian cancer cells grown in 2D cell culture.[23] Maloney et al. showed an increase in sensitivity toward NCT-505 when cells are grown in 3D cell culture, possibly due to the accompanying elevated levels of ALDH1A1 expression.[23] Elevated ALDH expression in 3D cell culture compared with 2D has also been described by others.[67,68] This phenomenon could be studied in more depth by looking at changes in the levels of active enzymes using **LEI-945**. Ferroptosis induced via GPX4 inhibition was synergistic with NCT-505-mediated toxicity. This combined therapy is of interest as both therapeutic targets, GPX4 and ALDH1A1, have been linked to therapy resistance in cancer.[56,59,60] Since both enzymes are involved in the detoxification of lipid peroxidation products, this might explain the observed synergistic effect.[69−71] Since NCT-505 inhibits also ALDH1A3, our data do not rule out the possibility that ALDH1A3 may also be an interesting drug target to tackle drug resistance in cancer. To conclude, **LEI-945** is a first-in-class retinal probe capable of the activity-based profiling of retinaldehyde dehydrogenases, which can be used for comparative and competitive ABPP of cancer cells and ALDH inhibitors, thereby providing guidance in the target validation and discovery of cancer (stem) cell-based therapies. Thus, these results showcase the application of substrate-based probes in interrogating pathologically relevant enzyme activities. They also highlight the general power of chemical proteomics in driving the discovery of new biological insights and guiding drug discovery efforts.

ASSOCIATED CONTENT

Ⓢ Supporting Information

The Supporting Information is available free of charge at https://pubs.acs.org/doi/10.1021/acscentsci.9b01022.

Detailed methods and protocols, chemical characterization, and proteomics data analysis (PDF)

Processed tables for LC-MS/MS measurement and analysis (XLSX)

AUTHOR INFORMATION

Corresponding Author
*E-mail: m.van.der.stelt@chem.leidenuniv.nl.

ORCID Ⓞ
Sebastiaan T. A. Koenders: 0000-0002-8486-4476
Lindsey Burggraaff: 0000-0002-2442-0443
Bob van de Water: 0000-0002-5839-2380
Mario van der Stelt: 0000-0002-1029-5717

Notes
The authors declare no competing financial interest.
The mass spectrometry proteomics data (raw data and IsoQuant output tables for proteins groups and peptides) have been deposited in the ProteomeXchange Consortium (http://proteomecentral.proteomexchange.org) via the PRIDE partner repository with the data set identifier PDX015495.[72,73]

REFERENCES

(1) Zile, M. H. Vitamin A and Embryonic Development: An Overview. *J. Nutr.* **1998**, *128* (2), 455S−458S.

(2) Wiseman, E. M.; Bar-El Dadon, S.; Reifen, R. The Vicious Cycle of Vitamin a Deficiency: A Review. *Crit. Rev. Food Sci. Nutr.* **2017**, *57* (17), 3703−3714.

(3) Mora, J. R.; Iwata, M.; von Andrian, U. H. Vitamin Effects on the Immune System. *Nat. Rev. Immunol.* **2008**, *8* (9), 685−698.

(4) Blomhoff, H. K.; Smeland, E. B.; Erikstein, B.; Rasmussen, A. M.; Skrede, B.; Skjonsberg, C.; Blomhoff, R. Vitamin A Is a Key Regulator for Cell Growth, Cytokine Production, and Differentiation in Normal B Cells. *J. Biol. Chem.* **1992**, *267* (33), 23988−23992.

(5) Carlberg, C. Lipid Soluble Vitamins in Gene Regulation. *BioFactors* **1999**, *10* (2−3), 91−97.

(6) Balmer, J. E.; Blomhoff, R. Gene Expression Regulation by Retinoic Acid. *J. Lipid Res.* **2002**, *43* (11), 1773−1808.

(7) D'Ambrosio, D. N.; Clugston, R. D.; Blaner, W. S. Vitamin A Metabolism: An Update. *Nutrients* **2011**, *3*, 63−103.

(8) Koppaka, V.; Thompson, D. C.; Chen, Y.; Ellermann, M.; Nicolaou, K. C.; Juvonen, R. O.; Petersen, D.; Deitrich, R. A.; Hurley, T. D.; Vasiliou, V. Aldehyde Dehydrogenase Inhibitors: A Comprehensive Review of the Pharmacology, Mechanism of Action, Substrate Specificity, and Clinical Application. *Pharmacol. Rev.* **2012**, *64* (3), 520−539.

(9) Duester, G.; Mic, F. A.; Molotkov, A. Cytosolic Retinoid Dehydrogenases Govern Ubiquitous Metabolism of Retinol to Retinaldehyde Followed by Tissue-Specific Metabolism to Retinoic Acid. In *Chemico-Biological Interactions*; Elsevier, 2003; Vol. *143−144*, pp 201−210, DOI: 10.1016/S0009-2797(02)00204-1.

(10) Luo, Y.; Dallaglio, K.; Chen, Y.; Robinson, W. A.; Robinson, S. E.; McCarter, M. D.; Wang, J.; Gonzalez, R.; Thompson, D. C.; Norris, D. A.; et al. ALDH1A Isozymes Are Markers of Human Melanoma Stem Cells and Potential Therapeutic Targets. *Stem Cells* **2012**, *30* (10), 2100−2113.

(11) Qiu, Y.; Pu, T.; Li, L.; Cheng, F.; Lu, C.; Sun, L.; Teng, X.; Ye, F.; Bu, H. The Expression of Aldehyde Dehydrogenase Family in Breast Cancer. *J. Breast Cancer* **2014**, *17* (1), 54−60.

(12) Sládek, N. E.; Kollander, R.; Sreerama, L.; Kiang, D. T. Cellular Levels of Aldehyde Dehydrogenases (ALDH1A1 and ALDH3A1) as Predictors of Therapeutic Responses to Cyclophosphamide-Based Chemotherapy of Breast Cancer: A Retrospective Study. *Cancer Chemother. Pharmacol.* **2002**, *49* (4), 309−321.

(13) Croker, A. K.; Allan, A. L. Inhibition of Aldehyde Dehydrogenase (ALDH) Activity Reduces Chemotherapy and Radiation Resistance of Stem-like ALDH HiCD44 + Human Breast Cancer Cells. *Breast Cancer Res. Treat.* **2012**, *133* (1), 75−87.

(14) Wang, J.; Nikhil, K.; Viccaro, K.; Chang, L.; White, J.; Shah, K. Phosphorylation-Dependent Regulation of ALDH1A1 by Aurora Kinase A: Insights on Their Synergistic Relationship in Pancreatic Cancer. *BMC Biol.* **2017**, *15* (10), 1−22.

(15) Zhao, D.; Mo, Y.; Li, M. T.; Zou, S. W.; Cheng, Z. L.; Sun, Y. P.; Xiong, Y.; Guan, K. L.; Lei, Q. Y. NOTCH-Induced Aldehyde Dehydrogenase 1A1 Deacetylation Promotes Breast Cancer Stem Cells. *J. Clin. Invest.* **2014**, *124* (12), 5453−5465.

(16) Moreb, J. S.; Zucali, J. R.; Ostmark, B.; Benson, N. A. Heterogeneity of Aldehyde Dehydrogenase Expression in Lung Cancer Cell Lines Is Revealed by Aldefluor Flow Cytometry-Based Assay. *Cytometry, Part B* **2007**, *72B* (4), 281−289.

(17) Marcato, P.; Dean, C. A.; Pan, D.; Araslanova, R.; Gillis, M.; Joshi, M.; Helyer, L.; Pan, L.; Leidal, A.; Gujar, S.; et al. Aldehyde Dehydrogenase Activity of Breast Cancer Stem Cells Is Primarily Due To Isoform ALDH1A3 and Its Expression Is Predictive of Metastasis. *Stem Cells* **2011**, *29* (1), 32−45.

(18) Zhou, L.; Sheng, D.; Wang, D.; Ma, W.; Deng, Q.; Deng, L.; Liu, S. Identification of Cancer-Type Specific Expression Patterns for Active Aldehyde Dehydrogenase (ALDH) Isoforms in ALDEFLUOR Assay. *Cell Biol. Toxicol.* **2019**, *35* (2), 161−177.

(19) Anorma, C.; Hedhli, J.; Bearrood, T. E.; Pino, N. W.; Gardner, S. H.; Inaba, H.; Zhang, P.; Li, Y.; Feng, D.; Dibrell, S. E.; et al. Surveillance of Cancer Stem Cell Plasticity Using an Isoform-Selective Fluorescent Probe for Aldehyde Dehydrogenase 1A1. *ACS Cent. Sci.* **2018**, *4* (8), 1045−1055.

(20) Yagishita, A.; Ueno, T.; Esumi, H.; Saya, H.; Kaneko, K.; Tsuchihara, K.; Urano, Y. Development of Highly Selective Fluorescent Probe Enabling Flow-Cytometric Isolation of ALDH3A1-Positive Viable Cells. *Bioconjugate Chem.* **2017**, *28* (2), 302−306.

(21) Yasgar, A.; Titus, S. A.; Wang, Y.; Danchik, C.; Yang, S. M.; Vasiliou, V.; Jadhav, A.; Maloney, D. J.; Simeonov, A.; Martinez, N. J. A High-Content Assay Enables the Automated Screening and Identification of Small Molecules with Specific ALDH1A1-Inhibitory Activity. *PLoS One* **2017**, *12* (1), 1−19.

(22) Koch, M. F.; Harteis, S.; Blank, I. D.; Pestel, G.; Tietze, L. F.; Ochsenfeld, C.; Schneider, S.; Sieber, S. A. Structural, Biochemical, and Computational Studies Reveal the Mechanism of Selective Aldehyde Dehydrogenase 1A1 Inhibition by Cytotoxic Duocarmycin Analogues. *Angew. Chem., Int. Ed.* **2015**, *54* (46), 13550−13554.

(23) Yang, S. M.; Martinez, N. J.; Yasgar, A.; Danchik, C.; Johansson, C.; Wang, Y.; Baljinnyam, B.; Wang, A. Q.; Xu, X.; Shah, P.; et al. Discovery of Orally Bioavailable, Quinoline-Based Aldehyde Dehydrogenase 1A1 (ALDH1A1) Inhibitors with Potent Cellular Activity. *J. Med. Chem.* **2018**, *61* (11), 4883−4903.

(24) Serwa, R.; Tate, E. W. Activity-Based Profiling for Drug Discovery. *Chem. Biol.* **2011**, *18*, 407−409.

(25) Cravatt, B. F.; Wright, A. T.; Kozarich, J. W. Activity-Based Protein Profiling: From Enzyme Chemistry to Proteomic Chemistry. *Annu. Rev. Biochem.* **2008**, *77* (1), 383−414.

(26) Liu, Y.; Patricelli, M. P.; Cravatt, B. F. Activity-Based Protein Profiling: The Serine Hydrolases. *Proc. Natl. Acad. Sci. U. S. A.* **1999**, *96* (26), 14694−14699.

(27) Van Esbroeck, A. C. M.; Janssen, A. P. A.; Cognetta, A. B.; Ogasawara, D.; Shpak, G.; Van Der Kroeg, M.; Kantae, V.; Baggelaar, M. P.; De Vrij, F. M. S.; Deng, H.; et al. Activity-Based Protein Profiling Reveals off-Target Proteins of the FAAH Inhibitor BIA 10−2474. *Science* **2017**, *356* (6342), 1084−1087.

(28) Cisar, J. S.; Weber, O. D.; Clapper, J. R.; Blankman, J. L.; Henry, C. L.; Simon, G. M.; Alexander, J. P.; Jones, T. K.; Ezekowitz, R. A. B.; O'Neill, G. P.; et al. Identification of ABX-1431, a Selective Inhibitor of Monoacylglycerol Lipase and Clinical Candidate for Treatment of Neurological Disorders. *J. Med. Chem.* **2018**, *61* (20), 9062−9084.

(29) Ahn, K.; Johnson, D. S.; Mileni, M.; Beidler, D.; Long, J. Z.; McKinney, M. K.; Weerapana, E.; Sadagopan, N.; Liimatta, M.; Smith, S. E.; et al. Discovery and Characterization of a Highly Selective FAAH Inhibitor That Reduces Inflammatory Pain. *Chem. Biol.* **2009**, *16* (4), 411−420.

(30) Baggelaar, M. P.; Janssen, F. J.; van Esbroeck, A. C. M.; den Dulk, H.; Allarà, M.; Hoogendoorn, S.; McGuire, R.; Florea, B. I.; Meeuwenoord, N.; van den Elst, H.; et al. Development of an Activity-Based Probe and In Silico Design Reveal Highly Selective Inhibitors for Diacylglycerol Lipase-*α* in Brain. *Angew. Chem., Int. Ed.* **2013**, *52* (46), 12081−12085.

(31) Serim, S.; Haedke, U.; Verhelst, S. H. L. Activity-Based Probes for the Study of Proteases: Recent Advances and Developments. *ChemMedChem* **2012**, *7*, 1146−1159.

(32) Zhao, Q.; Ouyang, X.; Wan, X.; Gajiwala, K. S.; Kath, J. C.; Jones, L. H.; Burlingame, A. L.; Taunton, J. Broad-Spectrum Kinase

(33) Kuo, C. L.; van Meel, E.; Kytidou, K.; Kallemeijn, W. W.; Witte, M.; Overkleeft, H. S.; Artola, M. E.; Aerts, J. M. Activity-Based Probes for Glycosidases: Profiling and Other Applications. *Methods Enzymol.* **2018**, *598*, 217−235.

(34) Morgan, C. A.; Hurley, T. D. Characterization of Two Distinct Structural Classes of Selective Aldehyde Dehydrogenase 1A1 Inhibitors. *J. Med. Chem.* **2015**, *58* (4), 1964−1975.

(35) Thiele, C.; Papan, C.; Hoelper, D.; Kusserow, K.; Gaebler, A.; Schoene, M.; Piotrowitz, K.; Lohmann, D.; Spandl, J.; Stevanovic, A.; et al. Tracing Fatty Acid Metabolism by Click Chemistry. *ACS Chem. Biol.* **2012**, *7* (12), 2004−2011.

(36) Gaebler, A.; Milan, R.; Straub, L.; Hoelper, D.; Kuerschner, L.; Thiele, C. Alkyne Lipids as Substrates for Click Chemistry-Based in Vitro Enzymatic Assays. *J. Lipid Res.* **2013**, *54* (8), 2282−2290.

(37) Surmatis, J. D.; Thommen, R. A Total Synthesis of Astaxanthin Dimethyl Ether. *J. Org. Chem.* **1967**, *32* (1), 180−184.

(38) Haugan, J. A.; Jansson, P.-E.; Lindqvist, B.; Andrei, G.; Snoeck, R.; Balzarini, J.; Fransson, B.; Ragnarsson, U.; Francis, G. W. Total Synthesis of C31-Methyl Ketone Apocarotenoids: Sintaxanthin and (3R)-3-Hydroxysintaxanthin. *Acta Chem. Scand.* **1994**, *48*, 657−664.

(39) Morgan, C. A.; Parajuli, B.; Buchman, C. D.; Dria, K.; Hurley, T. D. N,N-Diethylaminobenzaldehyde (DEAB) as a Substrate and Mechanism-Based Inhibitor for Human ALDH Isoenzymes. *Chem.-Biol. Interact.* **2015**, *234*, 18−28.

(40) Kang, J. H.; Lee, S. H.; Hong, D.; Lee, J. S.; Ahn, H. S.; Ahn, J. H.; Seong, T. W.; Lee, C. H.; Jang, H.; Hong, K. M.; et al. Aldehyde Dehydrogenase Is Used by Cancer Cells for Energy Metabolism. *Exp. Mol. Med.* **2016**, *48* (11), 1−13.

(41) Weerapana, E.; Wang, C.; Simon, G. M.; Richter, F.; Khare, S.; Dillon, M. B. D.; Bachovchin, D. A.; Mowen, K.; Baker, D.; Cravatt, B. F. Quantitative Reactivity Profiling Predicts Functional Cysteines in Proteomes. *Nature* **2010**, *468* (7325), 790−797.

(42) Notario, B. All-Trans-Retinoic Acid Binds to and Inhibits Adenine Nucleotide Translocase and Induces Mitochondrial Permeability Transition. *Mol. Pharmacol.* **2003**, *63* (1), 224−231.

(43) Dadsena, S.; Bockelmann, S.; Mina, J. G. M.; Hassan, D. G.; Korneev, S.; Razzera, G.; Jahn, H.; Niekamp, P.; Müller, D.; Schneider, M. Ceramides Bind VDAC2 to Trigger Mitochondrial Apoptosis. *Nat. Commun.* **2019**, *10* (1), 1832.

(44) Budelier, M. M.; Cheng, W. W. L.; Bergdoll, L.; Chen, Z. W.; Janetka, J. W.; Abramson, J.; Krishnan, K.; Mydock-McGrane, L.; Covey, D. F.; Whitelegge, J. P.; et al. Photoaffinity Labeling with Cholesterol Analogues Precisely Maps a Cholesterol-Binding Site in Voltage-Dependent Anion Channel-1. *J. Biol. Chem.* **2017**, *292* (22), 9294−9304.

(45) Rostovtseva, T. K.; Bezrukov, S. M. VDAC Regulation: Role of Cytosolic Proteins and Mitochondrial Lipids. *J. Bioenerg. Biomembr.* **2008**, *40* (3), 163−170.

(46) Ogata, H.; Goto, S.; Fujibuchi, W.; Kanehisa, M. Computation with the KEGG Pathway Database. *BioSystems* **1998**, *47* (1−2), 119−128.

(47) Bateman, A. UniProt: A Worldwide Hub of Protein Knowledge. *Nucleic Acids Res.* **2019**, *47* (1), 506−515.

(48) Thomas, P. D.; Kejariwal, A.; Campbell, M. J.; Mi, H.; Diemer, K.; Guo, N.; Ladunga, I.; Ulitsky-Lazareva, B.; Muruganujan, A.; Rabkin, S. PANTHER: A Browsable Database of Gene Products Organized by Biological Function, Using Curated Protein Family and Subfamily Classification. *Nucleic Acids Res.* **2003**, *31*, 334−341.

(49) Huang, D. W.; Sherman, B. T.; Lempicki, R. A. Systematic and Integrative Analysis of Large Gene Lists Using DAVID Bioinformatics Resources. *Nat. Protoc.* **2009**, *4* (1), 44−57.

(50) Tomita, H.; Tanaka, K.; Tanaka, T.; Hara, A. Aldehyde Dehydrogenase 1A1 in Stem Cells and Cancer. *Oncotarget* **2016**, *7* (10), 11018−11032.

(51) Beça, F. F. d.; Caetano, P.; Gerhard, R.; Alvarenga, C. A.; Gomes, M.; Paredes, J.; Schmitt, F. Cancer Stem Cells Markers

CD44, CD24 and ALDH1 in Breast Cancer Special Histological Types. *J. Clin. Pathol.* **2013**, *66* (3), 187−191.

(52) Hollestelle, A.; Nagel, J. H. A.; Smid, M.; Lam, S.; Elstrodt, F.; Wasielewski, M.; Ng, S. S.; French, P. J.; Peeters, J. K.; Rozendaal, M. J.; et al. Distinct Gene Mutation Profiles among Luminal-Type and Basal-Type Breast Cancer Cell Lines. *Breast Cancer Res. Treat.* **2010**, *121* (1), 53−64.

(53) Storms, R. W.; Trujillo, A. P.; Springer, J. B.; Shah, L.; Colvin, O. M.; Ludeman, S. M.; Smith, C. Isolation of Primitive Human Hematopoietic Progenitors on the Basis of Aldehyde Dehydrogenase Activity. *Proc. Natl. Acad. Sci. U. S. A.* **1999**, *96* (16), 9118−9123.

(54) Yoshida, A.; Hsu, L. C.; Dave, V. Retinal Oxidation Activity and Biological Role of Human Cytosolic Aldehyde Dehydrogenase. *Enzyme* **2017**, *46* (4−5), 239−244.

(55) Burgos, C.; de Burgos, N. M. G.; Rovai, L. E.; Blanco, A. In Vitro Inhibition by Gossypol of Oxidoreductases from Human Tissues. *Biochem. Pharmacol.* **1986**, *35* (5), 801−804.

(56) Raha, D.; Wilson, T. R.; Peng, J.; Peterson, D.; Yue, P.; Evangelista, M.; Wilson, C.; Merchant, M.; Settleman, J. The Cancer Stem Cell Marker Aldehyde Dehydrogenase Is Required to Maintain a Drug-Tolerant Tumor Cell Subpopulation. *Cancer Res.* **2014**, *74* (13), 3579−3590.

(57) Sakaue-Sawano, A.; Kurokawa, H.; Morimura, T.; Hanyu, A.; Hama, H.; Osawa, H.; Kashiwagi, S.; Fukami, K.; Miyata, T.; Miyoshi, H.; et al. Visualizing Spatiotemporal Dynamics of Multicellular Cell-Cycle Progression. *Cell* **2008**, *132* (3), 487−498.

(58) Dixon, S. J.; Lemberg, K. M.; Lamprecht, M. R.; Skouta, R.; Zaitsev, E. M.; Gleason, C. E.; Patel, D. N.; Bauer, A. J.; Cantley, A. M.; Yang, W. S.; et al. Ferroptosis: An Iron-Dependent Form of Nonapoptotic Cell Death. *Cell* **2012**, *149* (5), 1060−1072.

(59) Hangauer, M. J.; Viswanathan, V. S.; Ryan, M. J.; Bole, D.; Eaton, J. K.; Matov, A.; Galeas, J.; Dhruv, H. D.; Berens, M. E.; Schreiber, S. L.; et al. Drug-Tolerant Persister Cancer Cells Are Vulnerable to GPX4 Inhibition. *Nature* **2017**, *551* (7679), 247−250.

(60) Viswanathan, V. S.; Ryan, M. J.; Dhruv, H. D.; Gill, S.; Eichhoff, O. M.; Seashore-Ludlow, B.; Kaffenberger, S. D.; Eaton, J. K.; Shimada, K.; Aguirre, A. J.; et al. Dependency of a Therapy-Resistant State of Cancer Cells on a Lipid Peroxidase Pathway. *Nature* **2017**, *547* (7664), 453−457.

(61) Wright, A. T.; Cravatt, B. F. Chemical Proteomic Probes for Profiling Cytochrome P450 Activities and Drug Interactions In Vivo. *Chem. Biol.* **2007**, *14* (9), 1043−1051.

(62) Krysiak, J. M.; Kreuzer, J.; MacHeroux, P.; Hermetter, A.; Sieber, S. A.; Breinbauer, R. Activity-Based Probes for Studying the Activity of Flavin-Dependent Oxidases and for the Protein Target Profiling of Monoamine Oxidase Inhibitors. *Angew. Chem., Int. Ed.* **2012**, *51* (28), 7035−7040.

(63) Eleftheriadis, N.; Thee, S. A.; Zwinderman, M. R. H.; Leus, N. G. J.; Dekker, F. J. Activity-Based Probes for 15-Lipoxygenase-1. *Angew. Chem., Int. Ed.* **2016**, *55* (40), 12300−12305.

(64) Nesnas, N.; Rando, R. R.; Nakanishi, K. Synthesis of Biotinylated Retinoids for Cross-Linking and Isolation of Retinol Binding Proteins. *Tetrahedron* **2002**, *58* (32), 6577−6584.

(65) Jahng, W. J.; David, C.; Nesnas, N.; Nakanishi, K.; Rando, R. R. A Cleavable Affinity Biotinylating Agent Reveals a Retinoid Binding Role for RPE65. *Biochemistry* **2003**, *42* (20), 6159−6168.

(66) Marcato, P.; Dean, C. A.; Giacomantonio, C. A.; Lee, P. W. K. Aldehyde Dehydrogenase Its Role as a Cancer Stem Cell Marker Comes down to the Specific Isoform. *Cell Cycle* **2011**, *10*, 1378−1384.

(67) Reynolds, D. S.; Tevis, K. M.; Blessing, W. A.; Colson, Y. L.; Zaman, M. H.; Grinstaff, M. W. Breast Cancer Spheroids Reveal a Differential Cancer Stem Cell Response to Chemotherapeutic Treatment. *Sci. Rep.* **2017**, *7* (1), 1−12.

(68) Fujiwara, D.; Kato, K.; Nohara, S.; Iwanuma, Y.; Kajiyama, Y. The Usefulness of Three-Dimensional Cell Culture in Induction of Cancer Stem Cells from Esophageal Squamous Cell Carcinoma Cell Lines. *Biochem. Biophys. Res. Commun.* **2013**, *434* (4), 773−778.

(69) Yang, W. S.; Sriramaratnam, R.; Welsch, M. E.; Shimada, K.; Skouta, R.; Viswanathan, V. S.; Cheah, J. H.; Clemons, P. A.; Shamji, A. F.; Clish, C. B.; et al. Regulation of Ferroptotic Cancer Cell Death by GPX4. *Cell* **2014**, *156* (1−2), 317−331.

(70) Schneider, C.; Tallman, K. A.; Porter, N. A.; Brash, A. R. Two Distinct Pathways of Formation of 4-Hydroxynonenal. Mechanisms of Nonenzymatic Transformation of the 9- and 13-Hydroperoxides of Linoleic Acid to 4-Hydroxyalkenals. *J. Biol. Chem.* **2001**, *276* (24), 20831−20838.

(71) Yoval-Sánchez, B.; Rodríguez-Zavala, J. S. Differences in Susceptibility to Inactivation of Human Aldehyde Dehydrogenases by Lipid Peroxidation Byproducts. *Chem. Res. Toxicol.* **2012**, *25* (3), 722−729.

(72) Vizcaíno, J. A.; Deutsch, E. W.; Wang, R.; Csordas, A.; Reisinger, F.; Ríos, D.; Dianes, J. A.; Sun, Z.; Farrah, T.; Bandeira, N. ProteomeXchange Provides Globally Coordinated Proteomics Data Submission and Dissemination. *Nat. Biotechnol.* **2014**, *32*, 223−226.

(73) Perez-Riverol, Y.; Csordas, A.; Bai, J.; Bernal-Llinares, M.; Hewapathirana, S.; Kundu, D. J.; Inuganti, A.; Griss, J.; Mayer, G.; Eisenacher, M.; et al. The PRIDE Database and Related Tools and Resources in 2019: Improving Support for Quantification Data. *Nucleic Acids Res.* **2019**, *47* (1), 442−450.